mathematics

MDPI

Article

Coexisting Attractors in a Heterogeneous Agent Model in Discrete Time

Serena Brianzoni †, Giovanni Campisi *,† and Graziella Pacelli †

Department of Management, Polytechnic University of Marche, Piazzale Martelli 8, 60121 Ancona, Italy; s.brianzoni@staff.univpm.it (S.B.); g.pacelli@staff.univpm.it (G.P.)

* Correspondence: g.campisi@univpm.it

† These authors contributed equally to this work.

Abstract: In this paper, the discrete-time version of a continuous-time model with fundamentalists and momentum traders is presented. Our aim consists of studying the impact of cross-sectional momentum traders on the dynamics of the model. To this end, the continuous-time deterministic skeleton of the benchmark model is transformed using sophisticated discretization techniques. It is worth noting that the model does not always maintain the same characteristics after moving from continuous to discrete time. In spite of this, our discrete-time system preserves the dynamic properties of the continuous-time original model. Moreover, heterogeneity introduces an important non-linearity into the market dynamics, causing our deterministic financial model to generate erratic time series similar to the patterns observed in real markets. In particular, we show that the time series originated by the perturbed deterministic system capture some of the main stylized facts of the U.S. financial market. Converting the benchmark model from continuous time to discrete time allows the use of financial data available in discrete time.

Keywords: multi-asset; dynamical systems; heterogeneous agents; stochastic dynamics; stylized facts

MSC: 37N40; 37M05; 37M10; 37M15

Citation: Brianzoni, S.; Campisi, G.; Pacelli, G. Coexisting Attractors in a Heterogeneous Agent Model in Discrete Time. *Mathematics* **2023**, *11*, 2348. https://doi.org/10.3390/math11102348

Academic Editor: Davide Valenti

Received: 5 May 2023
Revised: 15 May 2023
Accepted: 16 May 2023
Published: 18 May 2023

1. Introduction

This paper explores the relevance of cross-sectional momentum traders to the stock market's return dynamics. The framework used is that of the heterogeneous agent model (HAM), which captures the qualitative pattern of the asset price in financial markets through the interaction of different types of agents that act according to specific trading rules (see, for example, [1–6]). The present paper analyzes a discrete-time version of the continuous-time model of [7], which includes different kinds of investors, to prove the time-varying economic dominance in financial markets. In particular, the time-varying dominance concerns the two controversial views of financial markets, that is, periods where they tend to be more efficient and periods where they tend to be less efficient. These two views are captured in [7] by considering three types of heterogeneous agents who trade multi-assets: fundamentalists, absolute momentum traders and cross-sectional momentum traders. Fundamentalists have a stabilizing role in the market; indeed, they believe that the price tends to its fundamental value (estimated considering various types of fundamental information). For this purpose, if the current price is above (or below) its fundamental value, fundamentalists place a selling (or buying) order since they believe that the price is overvalued (or undervalued). The model also includes two types of momentum traders who rely on extrapolative expectations and, unlike fundamentalists, have a destabilizing role in the market. Both types of momentum traders base their trading strategies on market conditions and historical prices instead of the fundamental value. However, while fundamentalists and absolute momentum traders invest only in one asset, cross-sectional traders invest in two assets simultaneously. It is the role of cross-sectional momentum

traders that leads the model to exhibit bistable dynamics. In fact, as in [7], our discrete-time model is also able to exhibit multiple attractors with very different structures. Depending on the initial price, the model can produce two opposing market phenomena that correspond to the two views of the financial market. In the first case (a more efficient financial market), the price tends to its equilibrium, while in the second case (a less efficient financial market), the deviations from the fundamental price are amplified by cross-sectional momentum traders, generating complex dynamics in the model.

The relevance of the model of [7] leads us to focus on a discrete-time version using a non-trivial discretization method scheme proposed by [8], called the nearly exact discretization scheme (NEDS). The method consists of transforming the original system of differential equations into an equivalent system of differential equations. The term equivalent means that when we consider the discretized model, the properties of the original model in continuous time have to be preserved. Beyond its simplicity, the choice of this method is also motivated by its efficacy. Indeed, this method has been applied in other works with successful results (see [9], for example).

Within the proposed model, this paper has two aims. The first is to apply the NEDS to the model of [7] and to prove that the resulting discrete-time model is dynamically consistent with the results obtained in its continuous-time counterpart. In this sense, we demonstrate that the qualitative dynamics do not change within our framework. Indeed, through the combination of analytical and numerical computations, we show that the results in terms of stability analysis are the same as those of the continuous-time model and that the same attractors, trajectories and bifurcations are obtained via numerical simulations. In particular, our model is able to generate the bistable dynamics observed in [7], and confirm the destabilizing role of cross-sectional momentum traders. This is an important result since discretized models often differ from the original ones in continuous time in terms of equilibria, their stability and bifurcations when it is known that discretization schemes should produce the same long-term behaviors as the original models. The second contribution to the literature concerns the application of the model to real financial data, which are usually available in discrete time. To this purpose, we show the ability of our discrete-time model to replicate various stylized facts of financial markets with reference to bubbles and crashes and volatility clustering phenomena, following the common approach in the literature (see, for example, [10,11]). Moreover, we take into account the importance of some parameters of the model that control the behavior of fundamentalists and cross-sectional traders, analyzing the reactions of these traders with respect to the path of the market's assets. We find that our results are in line with the evidence on these types of traders, confirming the stabilizing role of fundamentalists and the destabilizing role of cross-sectional momentum traders.

The paper is organized as follows. Section 2 presents the model and describes the discretization method applied. Section 3 explains how we conducted the local stability analysis and the related numerical simulations that confirmed the analytical results. Section 4 provides various numerical simulations of the stochastic version of the model, showing how it is able to match the patterns of the returns of several U.S. companies and the typical stylized facts documented in the literature, especially volatility clustering. Section 5 concludes.

2. The Model

We consider the model of multi-assets developed in continuous time published by [7]. Hence, in order to make the reading easier, let us recall the main aspects of the benchmark set-up.

The financial market of two risky assets A and B is populated by heterogeneous agents, i.e., fundamentalists and absolute and cross-sectional momentum traders, by introducing the following demand functions $\forall i, j = A, B$, $i \neq j$ (see the benchmark work of [7] for more details):

1. Fundamentalists : $D_{f,t} = \tanh[\beta_f(F_t^i - P_t^i)]$
2. Absolute momentum investors: $D_{a,t} = \tanh[\beta_a(P_t^i - P_{t-\tau}^i)]$

3. Cross-sectional momentum investors: $D^i_{c,t} = \tanh\Big\{\beta_c[(P^i_t - P^i_{t-\tau}) - (P^j_t - P^j_{t-\tau})]\Big\}$

where F^i_t and P^i_t are the log fundamental and market prices. In what follows, we assume that the fundamental price is constant, i.e., $F^i_t = F^i, \forall t$. The parameter $\beta_f > 0$ measures the mean reverting of market prices to their fundamental values, while parameters $\beta_a, \beta_c > 0$ capture the extrapolation rates on future prices of absolute and cross-sectional momentum investors, respectively. Notice that cross-sectional momentum traders focus on both assets simultaneously, which is different to the other traders who look at single assets.

By assuming constant fractions of different types of agents $\alpha^i_f, \alpha^i_a, \alpha^i_c > 0$ trading on asset i (constant proportions of the three types of traders satisfy: $\alpha^i_f + \alpha^i_a + \alpha^i_c = 1$, $\forall i = A, B$.), the authors arrive at the following final system:

$$\begin{aligned} P^i(t) = \frac{dP^i}{dt} =& \mu^i\big[\alpha^i_f \tanh\Big[\beta_f\Big(F^i - P^i(t)\Big)\Big] + \alpha^i_a \tanh\Big[\beta_a\Big(P^i(t) - P^i(t-\tau)\Big)\Big] + \\ &+ \alpha^i_c \tanh\Big\{\beta_c\Big[\Big(P^i(t) - P^i(t-\tau)\Big) - \Big(P^j(t) - P^j(t-\tau)\Big)\Big]\Big\}\big] \end{aligned} \tag{1}$$

where tanh denotes the hyperbolic tangent function, $i, j = A, B, \quad i \neq j$, $\mu^i > 0$ is the speed of the price adjustment made by the market maker, and the fundamental values F^i are assumed to be constant.

Our preliminary goal is the discretization of the model, i.e., to convert it into a discrete-time model. To achieve this, we make use of the non-trivial nearly exact discretization scheme (NEDS), as proposed by [8].

Our choice is due to the fact that this scheme captures and preserves the local stability and bifurcation of equilibrium points. In fact, the benchmark model admits a unique (fundamental) steady state whose local bifurcations are well investigated in continuous time. Hence, we are mainly interested in the analysis around it.

Moreover, its capability to allow for large time steps as well (which, in practice, can represent the period of some empirical measurements) (see again [8]) makes the method suitable for the present work, which aims at making use of real market data.

Finally, we appreciate its simplicity when compared to other schemes for moving from continuous to discrete time. The NEDS method and its properties are also well documented in [9], where the authors apply the NEDS to the Goodwin model.

Before proceeding, we expand the *tanh* by using the Taylor series, stopping at the third order: $tanh(x) = \tanh(x_0) + \tanh'(x_0)(x - x_0) + \frac{1}{2}\tanh''(x_0)(x - x_0)^2 + \frac{1}{6}\tanh'''(x_0)(x - x_0)^3 + o(x - x_0)^3$. Since System (1) has the unique fundamental steady state $(P^A, P^B) = (F^A, F^B)$, we use it as the center of the Taylor formula. We obtain $tanh(x) = x - \frac{1}{3}x^3 + o(x^3)$ (our mathematical approximations have sense in an opportune neighborhood of the fundamental steady state).

Hence, after expanding the *tanh* and posing $\tau = 1$, System (1) becomes:

$$\begin{aligned} \frac{dP^i}{dt} &= \gamma^i_f(F^i - P^i_t) + \gamma^i_a(P^i_t - P^i_{t-1}) + \gamma^i_c(P^i_t - P^i_{t-1}) - \gamma^i_c(P^j_t - P^j_{t-1}) + \\ &- \frac{1}{3}\mu^i\alpha^i_f\beta^3_f(F^i - P^i_t)^3 - \frac{1}{3}\mu^i\alpha^i_a\beta^3_a(P^i_t - P^i_{t-1})^3 - \frac{1}{3}\mu^i\alpha^i_c\beta^3_c[(P^i_t - P^i_{t-1}) - (P^j_t - P^j_{t-1})]^3 \end{aligned}$$

where we followed He et al. (2018) [7] in defining the measures of the activities of the three types of agents: $\gamma^i_f = \mu^i\alpha^i_f\beta_f$, $\gamma^i_a = \mu^i\alpha^i_a\beta_a$, $\gamma^i_c = \mu^i\alpha^i_c\beta_c$ $(i = A, B)$.

We now limit our considerations to the terms in prices until the second order (ignoring the third order terms) (notice that, in this way, the existence of the fundamental steady state is preserved) to obtain:

$$\frac{dP^i}{dt} = (\gamma^i_a + \gamma^i_c - \gamma^i_f)P^i_t - (\gamma^i_a + \gamma^i_c)P^i_{t-1} - \gamma^i_c P^j_t + \gamma^i_c P^j_{t-1} + \gamma^i_f F^i - \frac{1}{3}\mu^i\alpha^i_f\beta^3_f[-3P^i_t(F^i)^2 + 3F^i(P^i_t)^2]$$

that is:

$$\frac{dP^i}{dt} = (\gamma_a^i + \gamma_c^i - \gamma_f^i)P_t^i - (\gamma_a^i + \gamma_c^i)P_{t-1}^i - \gamma_c^i P_t^j + \gamma_c^i P_{t-1}^j + \gamma_f^i F^i - \mu^i \alpha_f^i \beta_f^3 \left[-P_t^i (F^i)^2 + F^i (P_t^i)^2\right] \quad (2)$$

For computational purposes, we rewrite the system in terms of deviations from fundamentals, $x_t^i = P_t^i - F^i$ (for $i = A, B$):

$$\frac{dx^i}{dt} = (\gamma_a^i + \gamma_c^i - \gamma_f^i)x_t^i - (\gamma_a^i + \gamma_c^i)x_{t-1}^i - \gamma_c^i(x_t^j - x_{t-1}^j) - \gamma_f^i \beta_f^2 \left[(F^i)^2 + F^i x_t^i\right] x_t^i \quad (3)$$

Let us move the derivative $\frac{dx}{dt}$ from continuous to discrete time by implementing the NEDS construction rules, as described by [8]:

- The left-hand side of the ODE is discretized in the following way:

$$\frac{dx}{dt} \to \frac{x_{t+1} - x_t}{\phi(h)}$$

  where h is the step size and $\phi(h) = h + O(h^2)\ as\ h \to 0^+$
- ϕ has the following form

$$\phi(h) = \frac{e^{rh} - 1}{r}$$

  with $r > 0$ real constant.

Notice that, in our case, coefficients of both equations of the system are the same. For this reason, the left-hand sides of both equations are discretized in the same way.

Applying this scheme to our ODE and considering that, in the right hand side of Equation (3), the term depending on x_t^i is of the form $r^i x_t^i + g(x_t^i)x_t^i$, we define $r^i = \gamma_a^i + \gamma_c^i - \gamma_f^i$ and $\phi^i(h) = \frac{e^{r^i h} - 1}{r^i}$ in order to obtain:

$$\frac{x_{t+1}^i - x_t^i}{\phi^i(h)} = r^i x_t^i - (\gamma_a^i + \gamma_c^i)x_{t-1}^i - \gamma_c^i(x_t^j - x_{t-1}^j) - \gamma_f^i \beta_f^2 [F^i x_t^i + (F^i)^2] x_t^i$$

which can be rewritten as:

$$x_{t+1}^i = r^i \frac{e^{r^i h} - 1}{r^i} x_t^i + x_t^i - \phi^i(h)\gamma_f^i \beta_f^2 [F^i x_t^i + (F^i)^2] x_t^i - \phi^i(h)(\gamma_a^i + \gamma_c^i)x_{t-1}^i - \phi^i(h)\gamma_c^i(x_t^j - x_{t-1}^j)$$

and we obtain the following final system:

$$x_{t+1}^i = e^{r^i h} x_t^i - \phi^i(h)\gamma_f^i \beta_f^2 [F^i x_t^i + (F^i)^2] x_t^i - \phi^i(h)(\gamma_a^i + \gamma_c^i)x_{t-1}^i - \phi^i(h)\gamma_c^i(x_t^j - x_{t-1}^j) \quad (4)$$

with $\phi^i(h) = \frac{e^{r^i h} - 1}{r^i}$, $r^i = \gamma_a^i + \gamma_c^i - \gamma_f^i$ and $h > 0$.

As previously explained, in this work we are interested in the dynamics around the fundamental steady state. Hence, let us now approach its local stability analysis.

3. Local Dynamics

In order to investigate the local stability of the unique fundamental steady state, we have to make use of technical variables for obtaining a system of first-order difference equations:

$$\begin{cases} x_{t+1}^A = e^{r^A h} x_t^A - \phi^A(h)\gamma_f^A \beta_f^2 [F^A x_t^A + (F^A)^2] x_t^A - \phi^A(h)(\gamma_a^A + \gamma_c^A)x_{t-1}^A - \phi^A(h)\gamma_c^A(x_t^B - x_{t-1}^B) \\ x_{t+1}^B = e^{r^B h} x_t^B - \phi^B(h)\gamma_f^B \beta_f^2 [F^B x_t^B + (F^B)^2] x_t^B - \phi^B(h)(\gamma_a^B + \gamma_c^B)x_{t-1}^B - \phi^B(h)\gamma_c^B(x_t^A - x_{t-1}^A) \\ y_{t+1}^A = x_t^A \\ y_{t+1}^B = x_t^B \end{cases} \quad (5)$$

whose Jacobian matrix evaluated at the fundamental equilibrium $(0, 0)$ is:

$$J(0,0) = \begin{pmatrix} e^{r^A h} - \phi^A(h)\gamma_f^A \beta_f^2 (F^A)^2 & -\phi^A(h)\gamma_c^A & -\phi^A(h)(\gamma_a^A + \gamma_c^A) & \phi^A(h)\gamma_c^A \\ -\phi^B(h)\gamma_c^B & e^{r^B h} - \phi^B(h)\gamma_f^B \beta_f^2 (F^B)^2 & \phi^B(h)\gamma_c^B & -\phi^B(h)(\gamma_a^B + \gamma_c^B) \\ 1 & 0 & 0 & 0 \\ 0 & 1 & 0 & 0 \end{pmatrix}.$$

We denote by $Det(J)$ and $Tr(J)$ the determinant and the trace of the Jacobian matrix J. The determinant is $Det(J) = \phi^A(h)\phi^B(h)[(\gamma_a^A + \gamma_c^A)(\gamma_a^B + \gamma_c^B) - \gamma_c^A \gamma_c^B]$ and the trace can be written as: $Tr(J) = 2 + (\gamma_a^A + \gamma_c^A)\phi^A(h) + (\gamma_a^B + \gamma_c^B)\phi^B(h) - \gamma_f^A \phi^A(h)[1 + (\beta_f F^A)^2] - \gamma_f^B \phi^B(h)[1 + (\beta_f F^B)^2]$ (we make use of relations $e^{r^i h} = r^i \phi^i(h) + 1$ and $r^i = \gamma_a^i + \gamma_c^i - \gamma_f^i$.).

Finally, we recall the necessary and sufficient conditions guaranteeing the local stability of fixed point:

$$1 + Tr(J) + Det(J) > 0$$

$$1 - Tr(J) + Det(J) > 0$$

$$1 - Det(J) > 0$$

and we remember that the violation of one of them implies, respectively, the "flip, fold and Neimark-Sacker" bifurcation (see [12]).

The stability conditions coming from the analytical study give us the chance to investigate the long-term behavior of the system by performing numerical simulations. In particular, the following numerical analysis aims at comparing the map with the benchmark model in continuous time.

To this end, we follow the definition given by [8], according to which a discretization scheme is dynamically consistent when the long-term behavior of the discrete model is the same as the continuous one, in terms of attractors and bifurcations.

Concerning the former, we first show that the discrete-time model is able to exhibit the same bistable dynamics as illustrated in [7]. To this end, in Figure 1, we plot the attractors of our system in the plane (x^A, x^B) for the same parameter values and initial conditions as the benchmark model. Our model exhibits the coexistence of attractors, and, as in [7], different price dynamics appear (for different initial values), and it also confirms the destabilizing role of cross-sectional momentum traders.

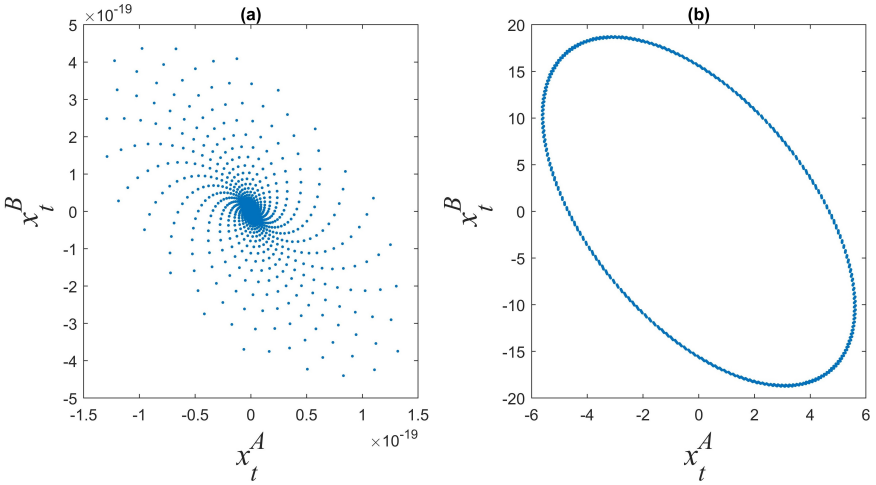

Figure 1. Attractor in the plane (x_t^A, x_t^B) for parameter values: $\alpha_f^A = 0.2$, $\alpha_f^B = 0.25$, $\alpha_c^A = 0.1$, $\alpha_c^B = 0.1$, $\beta_a = 0.05$, $\beta_c = 0.03$, $\mu^A = 15$, $\mu^B = 15$, $\beta_f = 0.2$, $\alpha_a^A = 0.7$, $\alpha_a^B = 0.65$, $F^A = 0$, $F^B = 0$, $\gamma_a^A = 0.6$, $\gamma_a^B = 0.75$, $\gamma_c^A = 0.045$, $\gamma_c^B = 0.045$, $\gamma_f^A = 0.6$, $\gamma_f^B = 0.75$, $r^A = 0.045$, $r^B = 0.045$, $\phi^A = 1.2559$, $\phi^B = 1.2559$, $h = 1.21$ and initial conditions $x_0^A = 2$, $x_0^B = 2$ in (**a**), while $x_0^A = 20$, $x_0^B = 20$ and $h = 1.2217$ in (**b**).

In order to show that the bifurcations of the ODE and DE are the same, in Figure 2, we depict the bifurcation diagram of the discrete variable x_t^A with respect to β_c, which shows the same bifurcations of [7] for the same range of the parameter β_c.

Finally, we recall that a discretization scheme is called a nearly exact discretization scheme if it is dynamically consistent and the trajectories of the resulting DE are the same or nearly the same as those of the ODE (see [8,9]). Hence, in Figure 3, we plot the trajectories of the continuous-time model of [7] (panel (a)) and the trajectories of our discrete-time model (panel (b)). As we can see, the trajectories are nearly the same for equal parameter values and initial conditions.

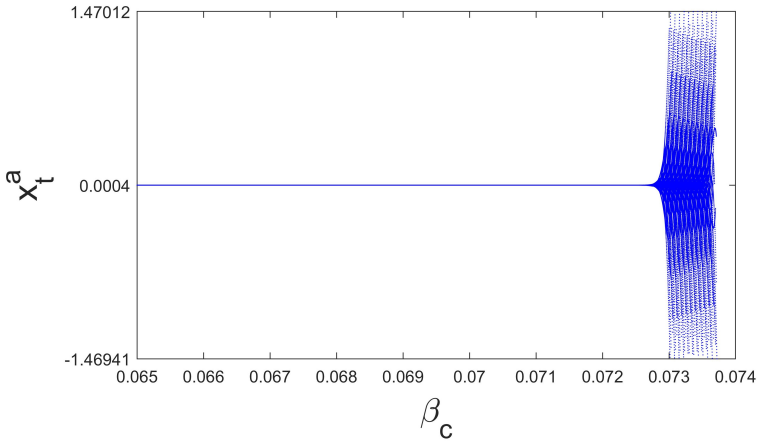

Figure 2. Bifurcation diagram on varying $\beta_c \in [0.065, 0.09]$ for parameter values: $\alpha_f^A = 0.2$, $\alpha_f^B = 0.25$, $\alpha_c^A = 0.1$, $\alpha_c^B = 0.1$, $\beta_a = 0.05$, $\mu^A = 15$, $\mu^B = 15$, $\beta_f = 0.2$, $\alpha_a^A = 0.7$, $\alpha_a^B = 0.65$, $F^A = 0$, $F^B = 0$, $\gamma_a^A = 0.6$, $\gamma_a^B = 0.75$, $\gamma_c^A = 0.045$, $\gamma_c^B = 0.045$, $\gamma_f^A = 0.6$, $\gamma_f^B = 0.75$, $r^A = 0.045$ $r^B = 0.045$, $\phi^A = 1.2559$, $\phi^B = 1.2559$, $h = 1.21$, and initial conditions $x_0^A = 2$, $x_0^B = 2$.

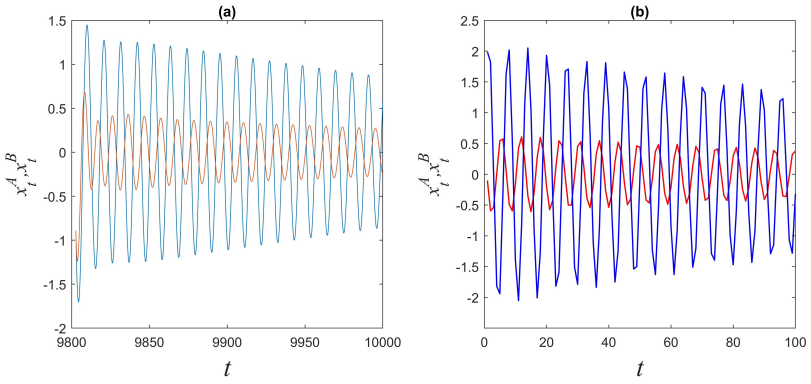

Figure 3. Comparison between continuous (panel (**a**)) and discrete (panel (**b**)) models for parameter values: $\alpha_f^A = 0.2$, $\alpha_f^B = 0.25$, $\alpha_c^A = 0.1$, $\alpha_c^B = 0.1$, $\beta_a = 0.05$, $\beta_c = 0.03$, $\mu^A = 15$, $\mu^B = 15$, $\beta_f = 0.2$, $\alpha_a^A = 0.7$, $\alpha_a^B = 0.65$, $F^A = 0$, $F^B = 0$, $\gamma_a^A = 0.6$, $\gamma_a^B = 0.75$, $\gamma_c^A = 0.045$, $\gamma_c^B = 0.045$, $\gamma_f^A = 0.6$, $\gamma_f^B = 0.75$, $r^A = 0.045$, $r^B = 0.045$, $\phi^A = 1.2559$, $\phi^B = 1.2559$, $h = 1.21$ and initial conditions $x_0^A = 2$, $x_0^B = 2$.

4. Empirical Model

In this section, we illustrate how our model is able to match some stylized facts of the U.S. market. We proceed in two steps. We first consider the assets of six of the biggest companies: Amazon (amzn), Apple (aapl), Tesla (tsla), Netflix (nflx), Exxon and Intel. Our dataset comes from Datastream and consists of 3082 daily observations starting in January 2003 and ending in February 2023. In what follows, the simulations are performed, including a stochastic component $\epsilon \sim N(0, (\sigma)^2)$, to the demand of each trader. σ is a positive parameter representing the standard deviations of the normal random variables

that we assume to be equal to one for all the traders. Numerical simulations focus on daily log returns, specified as:

$$r_t = \ln(P_t) - \ln(P_{t-1}) \tag{6}$$

In Figure 4, we present the time series of the returns of the six companies, while in Figure 5, we show the returns of the simulated time series of our model (Asset A and Asset B, respectively). Observing the two figures, we note that the path of the simulated time series reproduces the returns of the six companies. Both Figures 4 and 5 show that the time series exhibit volatility clustering, a phenomenon that highlights the occurrence of large fluctuations subsequently followed by small fluctuations in returns. Considering our model, assets A and B also show the phenomenon of fat tails in addition to that of volatility clustering, consistent with many empirical studies (see [13,14], for example).

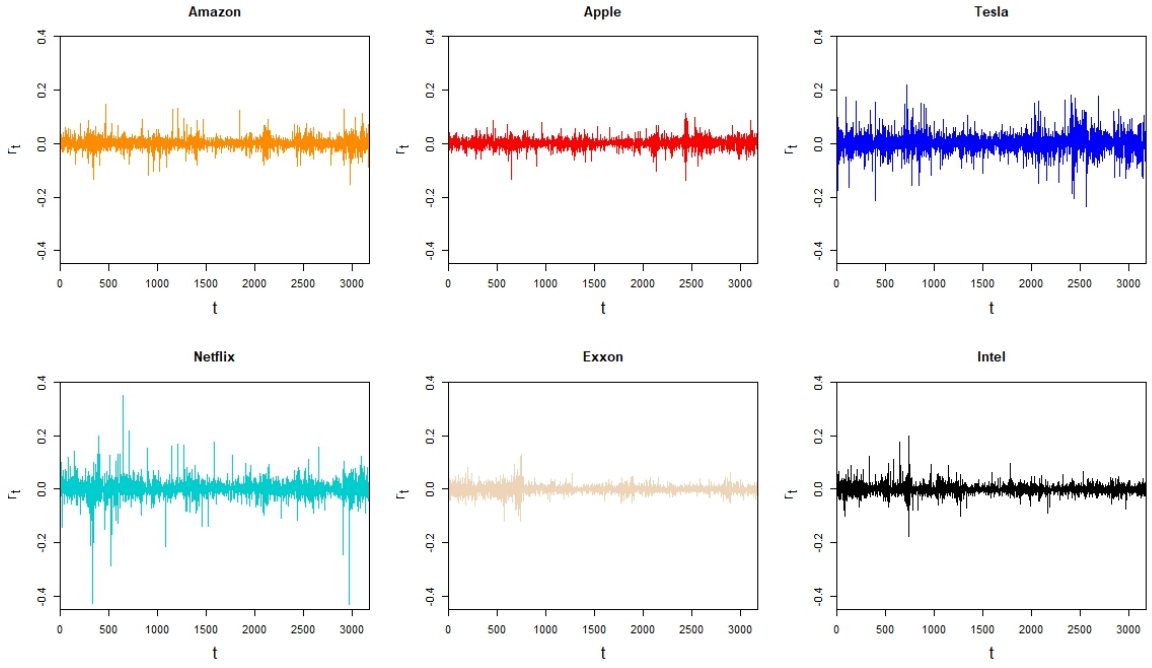

Figure 4. Volatility clustering. Empirical evidence from U.S. market.

In Table 1, we report some quantitative characteristics of the returns of the analyzed companies in the U.S. market; the same summary statistics were reported for our model. In our simulations, parameters are fixed, as in Figure 3. For convenience, we recall that $\beta_f = 0.2$ and $\beta_c = 0.03$, while initial conditions are $x_0^A = 2$, $x_0^B = 2$. The obtained results are reported in Table 1, where Assets A and B are similar to the couple Exxon–Tesla for what concerns the minimum and maximum of returns.

We also take into account changes in some key parameters. In particular, we focus on two parameters, β_f and β_c, which reflect the reactivity of the fundamentalists and cross-sectional momentum traders, respectively. The results are reported in Table 2 (for the fundamentalists) and Table 3 (for the cross-sectional momentum traders), where we varied only one parameter at a time. To this purpose, looking at Table 2, when β_f assumes the values of 0.2001 (see Figure 6) and 0.2003, the simulated model, including Assets A and B, is similar to the couple Exxon–Tesla. About the mean, increasing the value of β_f, we observe that, for $\beta_f = 0.2004$ and $\beta_f = 0.20044$, our model reproduces the statistics of the couples Intel–Netflix and Tesla–Netflix, respectively.

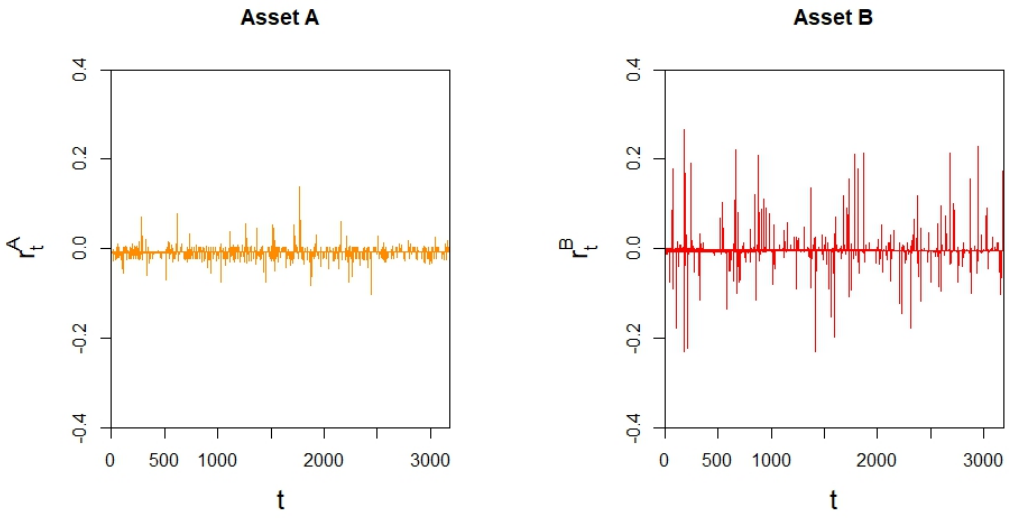

Figure 5. Volatility clustering. Asset A and Asset B of our model.

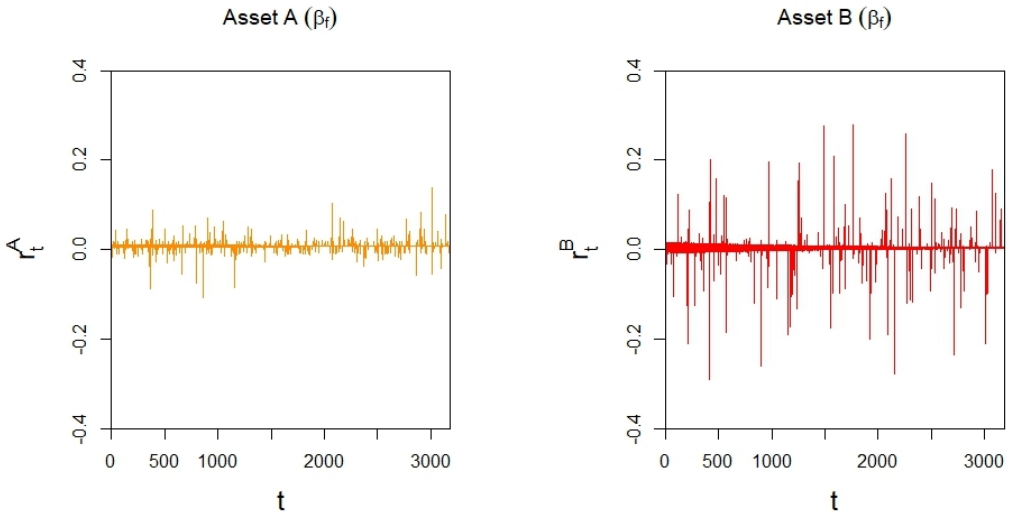

Figure 6. Volatility clustering. Asset A and Asset B of our model when $\beta_f = 0.2001$.

Table 1. Summary statistics of returns. The table reports the summary statistics including mean, standard deviation (sd), minimum and maximum values of Amazon, Apple, Tesla, Netflix, Exxon, Intel and Assets A and B.

Asset	Mean	sd	Min	Max
Amazon	0.0009	0.0205	−0.1514	0.1462
Apple	0.0008	0.0179	−0.1377	0.1132
Tesla	0.0016	0.0354	−0.2365	0.2183
Netflix	0.0009	0.0327	−0.4326	0.3522
Exxon	−0.0002	0.0162	−0.1194	0.1304
Intel	−0.0001	0.0188	−0.1783	0.1990
A	0.0084	0.0183	−0.1040	0.1376
B	−0.0039	0.0210	−0.2314	0.2662

From Table 2, we observe that, when increasing the values of β_f, the mean of both assets decreases, while maximum values increase and minimum values decrease, meaning that they trade more aggressively in order to bring the price to its equilibrium value. These results are coherent with the evidence on the behavior of fundamentalists (see, for

instance, [1,4]). In fact, fundamentalists tend to stabilize the market, and they bet on the mean reversion of the price to its fundamental value. However, the larger the mispricing, the more aggressive they become.

Table 2. Summary statistics of returns. The table reports the summary statistics, including mean, standard deviation (sd), and minimum and maximum values of Assets A and B when we only let β_f vary.

β_f	Asset	Mean	sd	Min	Max
0.2001	A	−0.0006	0.0081	−0.1074	0.1391
	B	0.0030	0.0232	−0.2898	0.2794
0.2003	A	−0.0007	0.0199	−0.1158	0.1448
	B	0.0029	0.0638	−0.2979	0.2960
0.2004	A	−0.0009	0.0685	−0.1442	0.1589
	B	0.0023	0.2220	−0.3219	0.3130
0.20044	A	−0.0101	0.1185	−0.2509	0.2150
	B	0.0004	0.3886	−0.6522	0.6488

On the other hand, considering the effects of the change in β_c, in Figure 7, we report the behavior of Assets A and B for $\beta_c = 0.03018$, while Table 3 describes their statistics when β_c varies. In particular, we can observe that, when increasing the values of the parameter β_c, the mean of Asset A always increases, while the mean of Asset B shows fluctuations (also, for what concerns minimum and maximum values, we observe fluctuations). This is in line with the behavior of momentum traders and System (5). Indeed, β_c exhibits anomalous behavior due to the fact that it influences both of the assets in System (5).

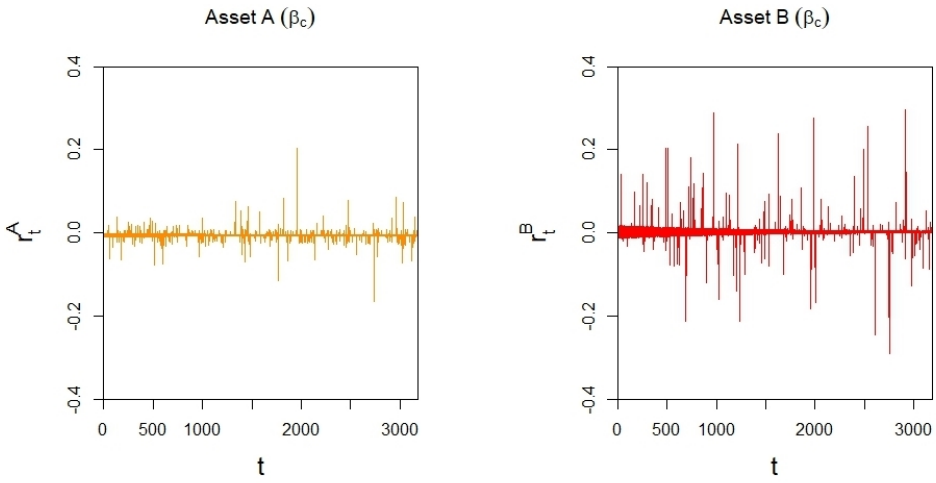

Figure 7. Volatility clustering. Asset A and Asset B of our model when $\beta_c = 0.03018$.

Finally, we would like to point out that we also checked the effect of changes in the parameter β_a, finding that it does not affect the path of the returns, as we expected.

We further investigated the phenomenon of volatility clustering from a quantitative perspective, following [10,11]. In detail, in order to observe the persistence of volatility, we performed an estimation of the power law component of autocorrelations (ACFs) of absolute returns, d. The results are shown in Table 4. We denote with q the number of lags, ζ the parameter capturing the ACF of absolute returns with lag one, and with d the power exponent capturing the decay of the ACFs. In line with [10,11], the value of d ranges between 0.2 and 0.4, confirming not only the presence of volatility clustering but also that our model is coherent with the stylized facts of four of the U.S. companies. However, it is worth noting that, about estimates of both Assets A and B, the value of R^2 is lower with

respect to the U.S. companies. Moreover, the significance level is also different among two assets. Indeed, the estimate of the parameter ζ is significant at 10% level for Asset A and at 1% for Asset B. Although our results do not replicate the stylized facts of U.S. companies perfectly, the model helps us understand the mechanism behind financial markets when traders with different investing attitudes interact. In this line of reasoning, our model does not represent a "facsimile model" whose purpose is to replicate some specific situations and "predict" the future exactly, but it intends to grasp the mechanism behind financial markets, and in this sense, it represents an abstract model useful to this scope in contrast to more complex models that prevent the understanding of such mechanisms (see [15,16] for a detailed discussion).

Table 3. Summary statistics of returns. The table reports the summary statistics, including mean, standard deviation (sd), and minimum and maximum values of Assets A and B when we let only β_c vary.

β_c	Asset	Mean	sd	Min	Max
0.0301	A	−0.0008	0.0089	−0.1067	0.1382
	B	−0.0039	0.0233	−0.2435	0.2719
0.03018	A	−0.0006	0.0092	−0.1647	0.2038
	B	0.0020	0.0221	−0.2916	0.2967
0.03025	A	0.0007	0.0096	−0.1349	0.1109
	B	0.0005	0.0248	−0.2971	0.2617
0.0305	A	0.0203	0.0277	−0.1445	0.1765
	B	0.0004	0.0843	−0.3041	0.2875

Table 4. Persistence of ACFs of absolute returns. For each return series in amzn, aapl, nflx, tsla, exxon, intel and Asset A and Asset B, we estimate $corr(|r_{t+q}|, |r_t|) \simeq \zeta / q^d$ with nonlinear least squares and report ζ and d [1].

	d	ζ	N	R^2
amzn $corr(\|r_{t+q}\|, \|r_t\|)$	0.2858 ***	0.1775 ***	60	0.6632
	(0.0206)			
aapl $corr(\|r_{t+q}\|, \|r_t\|)$	0.3955 ***	0.2408 ***	60	0.6729
	(0.0523)			
nflx $corr(\|r_{t+q}\|, \|r_t\|)$	0.2417 ***	0.1118 ***	60	0.3827
	(0.0284)			
tsla $corr(\|r_{t+q}\|, \|r_t\|)$	0.2820 ***	0.1581 ***	60	0.6022
	(0.0250)			
exxon $corr(\|r_{t+q}\|, \|r_t\|)$	0.2069 ***	0.3816 ***	60	0.7709
	(0.0317)			
intel $corr(\|r_{t+q}\|, \|r_t\|)$	0.3820 ***	0.2855 ***	60	0.7716
	(0.0412)			
Asset A $corr(\|r_{t+q}\|, \|r_t\|)$	0.3799 **	0.2118 *	60	0.1890
	(0.1700)			
Asset B $corr(\|r_{t+q}\|, \|r_t\|)$	0.3599 ***	0.2571 ***	60	0.2672
	(0.0812)			

[1] *** significant at 1%, ** significant at 5%, * significant at 10%.

5. Conclusions

We analyzed a discrete-time heterogeneous agent model based on the continuous-time counterpart investigated by [7]. We first discretized the model of [7] by making use of the nearly exact discretization scheme developed by [8] for its simplicity and relying on the successful results obtained. Then, we proved that our model preserves the same dynamics as the original continuous-time model. Indeed, it confirmed the bistable dynamics with the coexistence of multiple attractors. The use of this non-trivial discretization method enabled us to obtain a model that preserves the original dynamic properties in continuous time, in the sense of equilibria, their stability and bifurcations. The additional capability of our model with respect to the benchmark one is the possibility of making use of discrete-time data, as they are usually available in finance. Moreover, we also confirmed the destabilizing role of cross-sectional momentum traders in generating complex dynamics in the time series of returns. In addition, we considered a stochastic version of our model to capture the main stylized facts of the U.S. market. In particular, we focused on fat tails and the volatility clustering phenomenon. Finally, we concentrated our analysis on the effects of the key parameters on the pattern of returns, i.e., fundamentalists and cross-sectional momentum reactivity parameters. From numerical simulations, the results showed the stabilizing role of fundamentalists and the destabilizing role of cross-sectional momentum traders. The model lends itself to various extensions. In fact, we considered fixed proportions of agents, but the model can be extended by relaxing this assumption and analyzing the effects of some switching mechanisms (such as, for example, [2,6,17]). Another direction of future research should consider a more rigorous analysis of the stochastic part of the model, following the contributions of [18,19].

Author Contributions: Formal analysis, S.B.; investigation, S.B. and G.C.; software, G.C.; supervision, G.P.; validation, G.P.; visualization, G.P.; writing—original draft, S.B. and G.C.; writing—review and editing, S.B., G.C. and G.P. All authors have read and agreed to the published version of the manuscript.

Funding: This research received no external funding.

Data Availability Statement: The data presented in this study are available on request from the corresponding author.

Conflicts of Interest: The authors declare no conflict of interest.

References

1. Day, R.H.; Huang, W. Bulls, bears and market sheep. *J. Econ. Behav. Organ.* **1990**, *14*, 299–329. [CrossRef]
2. Brock, W.A.; Hommes, C.H. Heterogeneous beliefs and routes to chaos in a simple asset pricing model. *J. Econ. Dyn. Control* **1998**, *22*, 1235–1274. [CrossRef]
3. Bischi, G.I.; Gallegati, M.; Gardini, L.; Leombruni, R.; Palestrini, A. Herd behavior and nonfundamental asset price fluctuations in financial markets. *Macroecon. Dyn.* **2006**, *10*, 502–528. [CrossRef]
4. Tramontana, F.; Gardini, L.; Dieci, R.; Westerhoff, F. The emergence of bull and bear dynamics in a nonlinear model of interacting markets. *Discret. Dyn. Nat. Soc.* **2009**, *2009*, 310471.
5. Brianzoni, S.; Mammana, C.; Michetti, E. Updating wealth in an asset pricing model with heterogeneous agents. *Discret. Dyn. Nat. Soc.* **2010**, *2010*, 676317. [CrossRef]
6. Dieci, R.; He, X.Z. Cross-section instability in financial markets: Impatience, extrapolation, and switching. *Decis. Econ. Financ.* **2021**, *44*, 727–754. [CrossRef]
7. He, X.Z.; Li, K.; Wang, C. Time-varying economic dominance in financial markets: A bistable dynamics approach. *Chaos Interdiscip. J. Nonlinear Sci.* **2018**, *28*, 055903. [CrossRef] [PubMed]
8. Kwessi, E.; Elaydi, S.; Dennis, B.; Livadiotis, G. Nearly exact discretization of single species population models. *Nat. Resour. Model.* **2018**, *31*, e12167. [CrossRef]
9. Grassetti, F.; Guzowska, M.; Michetti, E. A dynamically consistent discretization method for Goodwin model. *Chaos Solitons Fractals* **2020**, *130*, 109420. [CrossRef]
10. He, X.Z.; Zheng, H. Trading heterogeneity under information uncertainty. *J. Econ. Behav. Organ.* **2016**, *130*, 64–80. [CrossRef]
11. Campisi, G.; Muzzioli, S.; Zaffaroni, A. Nonlinear dynamics in asset pricing: The role of a sentiment index. *Nonlinear Dyn.* **2021**, *105*, 2509–2523. [CrossRef]
12. Medio, A.; Lines, M. *Nonlinear Dynamics: A Primer*; Cambridge University Press: Cambridge, UK, 2001.

13. Lux, T. The socio-economic dynamics of speculative markets: Interacting agents, chaos, and the fat tails of return distributions. *J. Econ. Behav. Organ.* **1998**, *33*, 143–165. [CrossRef]
14. Chiarella, C.; Iori, G. A simulation analysis of the microstructure of double auction markets. *Quant. Financ.* **2002**, *2*, 346. [CrossRef]
15. Gilbert, N. *Agent-Based Models*; Sage Publications: Thousand Oaks, CA, USA, 2019.
16. Weisberg, M. *Simulation and Similarity: Using Models to Understand the World*; Oxford University Press: Oxford, UK, 2012.
17. Westerhoff, F.H.; Dieci, R. The effectiveness of Keynes–Tobin transaction taxes when heterogeneous agents can trade in different markets: A behavioral finance approach. *J. Econ. Dyn. Control* **2006**, *30*, 293–322. [CrossRef]
18. Franke, R.; Westerhoff, F. Why a simple herding model may generate the stylized facts of daily returns: Explanation and estimation. *J. Econ. Interact. Coord.* **2016**, *11*, 1–34. [CrossRef]
19. Kukacka, J.; Barunik, J. Estimation of financial agent-based models with simulated maximum likelihood. *J. Econ. Dyn. Control* **2017**, *85*, 21–45. [CrossRef]